Biomedicine & Pharmacotherapy 162 (2023) 114628

Contents lists available at ScienceDirect

Biomedicine & Pharmacotherapy

journal homepage: www.elsevier.com/locate/biopha

Ivacaftor therapy post myocardial infarction augments systemic inflammation and evokes contrasting effects with respect to tissue inflammation in brain and lung

Lotte Vanherle [a,b], Frank Matthes [a,b,c], Franziska E. Uhl [a,b], Anja Meissner [a,b,c,*]

[a] Department of Experimental Medical Science, Lund University, Lund, Sweden
[b] Wallenberg Centre for Molecular Medicine, Lund University, Lund, Sweden
[c] Department of Physiology, Institute for Theoretical Medicine, University of Augsburg, Augsburg, Germany

ARTICLE INFO

Keywords:
Myocardial infarction
Cystic fibrosis transmembrane regulator
Ivacaftor
Inflammation
Target tissue damage

ABSTRACT

Acquired cystic fibrosis transmembrane regulator (CFTR) dysfunctions have been associated with several conditions, including myocardial infarction (MI). Here, CFTR is downregulated in brain, heart, and lung tissue and associates with inflammation and degenerative processes. Therapeutically increasing CFTR expression attenuates these effects. Whether potentiating CFTR function yields similar beneficial effects post-MI is unknown. The CFTR potentiator ivacaftor is currently in clinical trials for treatment of acquired CFTR dysfunction associated with chronic obstructive pulmonary disease and chronic bronchitis. Thus, we tested ivacaftor as therapeutic strategy for MI-associated target tissue inflammation that is characterized by CFTR alterations.

MI was induced in male C57Bl/6 mice by ligation of the left anterior descending coronary artery. Mice were treated with ivacaftor starting ten weeks post-MI for two consecutive weeks.

Systemic ivacaftor treatment ameliorates hippocampal neuron dendritic atrophy and spine loss and attenuates hippocampus-dependent memory deficits occurring post-MI. Similarly, ivacaftor therapy mitigates MI-associated neuroinflammation (i.e., reduces higher proportions of activated microglia). Systemically, ivacaftor leads to higher frequencies of circulating $Ly6C^{+}$ and $Ly6C^{hi}$ cells compared to vehicle-treated MI mice. Likewise, an ivacaftor-mediated augmentation of MI-associated pro-inflammatory macrophage phenotype characterized by higher CD80-positivity is observed in the MI lung. *In vitro,* ivacaftor does not alter LPS-induced CD80 and tumor necrosis factor alpha mRNA increases in BV2 microglial cells, while augmenting mRNA levels of these markers in mouse macrophages and differentiated human THP-1-derived macrophages.

Our results suggest that ivacaftor promotes contrasting effects depending on target tissue post-MI, which may be largely dependent on its effects on different myeloid cell types.

1. Introduction

Structural and functional alterations of the cystic fibrosis transmembrane conductance regulator (CFTR) are well-recognized in cystic fibrosis (CF) [1]. More recently, the channel has gained interest in the pathophysiology of other chronic lung diseases, such as chronic obstructive pulmonary disease (COPD) [2–4], asthma [3] and chronic bronchitis [2] where acquired CFTR alterations have been reported.

Although the expression of CFTR is not limited to the lung [5–8], the role of acquired CFTR deficiency in the course of various diseases in non-CF individuals has only recently been investigated. With regard to non-CF airway pathologies, a number of environmental insults including, cigarette smoke, hypoxia, and inflammation have been reported to promote chronic rhinosinusitis, COPD, chronic bronchitis, and asthma by inducing acquired CFTR dysfunction [9–16]. Specifically, tobacco smoke has been associated with systemic CFTR dysfunction [14,17,18]. Similarly, heart failure experimentally induced by myocardial infarction (MI) associates with CFTR downregulation in multiple organs, including the heart, the lung, and the brain [6] with serious implications for tissue structure and function [19–22].

Abbreviations: CFTR –, cystic fibrosis transmembrane regulator; Iva –, ivacaftor; Lum –, lumacaftor; MI –, myocardial infarction.

* Correspondence to: Klinikgatan 32, SE-22184 Lund, Sweden.
E-mail addresses: lotte.vanherle.8386@med.lu.se (L. Vanherle), frank.matthes@med.lu.se (F. Matthes), franziuhl82@gmail.com (F.E. Uhl), anja.meissner@med.lu.se (A. Meissner).

https://doi.org/10.1016/j.biopha.2023.114628
Received 10 February 2023; Received in revised form 27 March 2023; Accepted 29 March 2023
Available online 3 April 2023

In CF patients, CFTR defects can therapeutically be targeted by small molecules acting as CFTR potentiators, correctors or amplifiers. Combination treatments including the CFTR potentiator ivacaftor and CFTR correctors such as lumacaftor, tezacaftor or elexacaftor are widely used. At present, the potentiator ivacaftor (marketed as Kalydeco®) is the only FDA approved CFTR modulator monotherapy for CF patients with a G551D mutation (i.e., 2.5–5% of all CF patients [23]). Besides that, ivacaftor is currently in several clinical trials for the treatment of various pulmonary diseases with an acquired CFTR dysfunction, including COPD and chronic bronchitis [2–4]. In animal models, acquired systemic CFTR downregulation post-MI is improved after C18, lumacaftor and lumacaftor/ivacaftor therapy [19,20]. Specifically, CFTR corrector compound-induced increases in neuronal CFTR expression ameliorate structural alterations in hippocampal neurons and memory impairment post-MI (10). Lumacaftor therapy further attenuates MI-associated adverse vascular remodeling of the lung and reduces pulmonary inflammation by promoting favorable polarization of non-alveolar macrophages [22].

Thus, targeting such acquired CFTR dysfunction in airway and non-airway related diseases in non-CF settings represents a novel treatment strategy that may benefit a larger patient population beyond the CF field. Moreover, prices for the marketed CFTR modulator drugs are high [24], creating additional value for the investigation regarding the drugs' repurposing potential in order to increase drug demand and therefore, potentially reduce production cost. Considering first promising results with regard to lung function from clinical ivacaftor trials in acquired airway CFTR dysfunction [2], the current study tests its efficacy in MI-induced target tissue injury that is characterized by CFTR alterations [6,19–22].

2. Material and methods

2.1. Materials

All chemicals used were purchased from Fisher Scientific (Gothenburg, Sweden), Saveen & Werner (Limhamn, Sweden), Sigma-Aldrich (Stockholm, Sweden), or Nordic Biosite (Täby, Sweden) unless otherwise stated. Primers utilized for qPCR were purchased from Eurofins (Ebersberg, Germany).

2.2. Ethics approval

The current investigation conforms to the EU Directive 2010/63/EU for animal experiments and the ARRIVE 2.0 guidelines. The study, approved by the institutional ethical committee for animal experiments Malmö/Lund (Dnr 5.8.18–04938/2021), was performed according to the Swedish Animal welfare ACT SFS 1988:534 act and conducted in accordance with European animal protection laws.

2.3. Animals

Male wild-type (WT) C57Bl/6 N mice purchased from Taconic Biosciences (Ejby, Denmark) were used and housed under a standard 12 h:12 h light-dark cycle in a climate-controlled facility, fed normal chow and had access to food and water ad libitum. Surgical procedures were conducted on 12-week-old mice with a body weight $\geq$ 25 g.

2.4. Induction of myocardial infarction in mice

A left anterior descending (LAD) coronary artery ligation was used to induce an MI as described previously [20–22]. Briefly, mice were anesthetized with 2–3% isoflurane (IsoFlo in room air; Abbott, Solna, Sweden) before they were intubated with a 22-gauge angiocatheter (BD, Helsingborg, Sweden), and were ventilated at a rate of 120 breaths per minute with a 200–250 μl tidal volume and 3 cm positive end expiratory pressure (MiniVent; Hugo Sachs, March, Germany). Following a left lateral thoracotomy, the pericardium was opened, and the LAD was permanently ligated with 7–0 non-absorbable suture (AgnTho's; Lidingö, Sweden). Thereafter, the chest was closed, and upon restoration of spontaneous respiration, mice were extubated. Post-surgery, all mice received buprenorphine (0.05 mg/kg delivered subcutaneously every twelve hours for 2–4 times).

Animals were assigned to the following treatment groups at 10 weeks post-surgery: MI + vehicle (ctrl; 10% DMSO in 50:50 PEG/H_2O); MI + ivacaftor (1.875 mg/kg ivacaftor in 10% DMSO / 90% 50:50 PEG/H_2O); or MI + lumacaftor (3 mg/kg lumacaftor in 10% DMSO / 90% 50:50 PEG/H_2O). Dosages are based on previously published data [19,20]. The treatments were administered by intraperitoneal (i.p.) injection daily for 2 consecutive weeks, starting 10 weeks after MI induction. At endpoint, mice were euthanized under 2% isoflurane anesthesia for tissue collection. This study contains data from 2 different MI cohorts: [1] 3 months post-MI with ivacaftor treatment (N = 8 MI + vehicle, N = 8 MI + Iva); and [2] 3 months post-MI with lumacaftor treatment (N = 8 MI + vehicle, N = 10 MI + Lum).

2.5. Novel object recognition test

A novel object recognition test with a 1-hour delay interval was used to assess hippocampal non-spatial memory that involves the activation of CA1 neurons [25,26], as previously described [20]. Briefly, habituated mice were allowed to explore two identical objects for 8 min. On the test day, mice were re-exposed to the same identical objects. After one hour, one of the original objects was exchanged for a novel object and mice were allowed to explore the two objects for 8 min. Both, objects and arena were thoroughly cleaned with 70% ethanol between each test, to eliminate potential odor cues. Mice were video tracked with AnyMaze software (Stoelting; Dublin, Ireland); time spent exploring the novel (Tn) and the original (To) object were recorded. The results were verified by manual Tn and To determination using stopwatches by an observer blinded to the experimental group assignments. A recognition index (RI) was calculated from Tn/[Tn+To]. Animals with total exploration times below 20 s were excluded from analyses.

2.6. Fluorescence activated cell sorting (FACS)

After whole blood collection and trans-cardiac perfusion, lung-heart blocks were extracted, and broncho-alveolar lavage was performed by instillation of sterile PBS. The left lung was mechanically dissociated into pieces and enzymatically digested in a DNAse-Collagenase XI mix under continuous agitation. After centrifugation and red blood cell (RBC) lysis, the cell pellets were reconstituted in Fc block (1:100 in FACS buffer; phosphate buffered saline (PBS) + 2% fetal bovine serum (FBS) + 2 mM ethylenediaminetetraacetic acid (EDTA); pH 7.4) prior to antibody staining (Supplemental Table 1) [22]. From whole blood, RBCs were lysed, and cell pellets were incubated in Fc block (1:100 in FACS buffer) prior to staining with antibodies for 30 min at 4 °C (Supplemental Table 1). Samples were washed with FACS buffer to remove the antibody solution and centrifuged at 400xg at 4 °C for 5 min prior to resuspension in FACS buffer. Data acquisition was carried out on a BD LSR Fortessa cytometer using FacsDiva software Vision 8.0 (BD Biosciences). Data analysis was performed with FlowJo software (version 10, TreeStar Inc., Ashland, OR, USA). Cells were plotted on forward versus side scatter and single cells were gated on FSC-A versus FSC-H linearity.

2.7. Immunofluorescence analyses

Coronal brain sections (10 μm) were stained with ionized calcium-binding adapter molecule-1 (Iba-1; FUJIFILM Wako Shibayagi Cat# 019–19741, Supplemental Table 1) in a humidity chamber over night at 4 °C after blocking with a blocking reagent (Roche). Slides were washed with PBS, incubated with secondary antibody (Supplemental Table 1)

for 1 h at room temperature, and mounted with Fluoromount-G with DAPI. In brain slices, CA1 and DG Iba-1 + microglia were classified based on morphology into ramified (resting state; cells with a small cell body and long processes), intermediate (cells with enlarged cell body and thickened, reduced branches), and round (active state; cells with round cell body without visible branches) [27]. Representative images were generated with a Nikon A1RHD confocal microscope.

2.8. Histological analysis of dendrite morphology

Neuronal arborization and dendritic spine density of pyramidal neurons of the hippocampus were assessed in coronal Golgi-Cox-stained brain sections (150 μm) as previously described [20,28,29]. Neurons and their dendritic spines were imaged with a Nikon Eclipse Ti2 microscope (Nikon Instruments Europe) and analyzed using Image J (https://imagej.net/ Sholl_Analysis, version 3.7.4). The arborization of single hippocampal neurons from CA1 region were digitally assessed from hyperstack images using the Simple Neurite Tracer plugin for Image J and analyzed using Sholl analysis [30]. The center of the soma was pinpointed, and arborization was then characterized by Sholl analysis (https://imagej.net/Sholl_Analysis, version 3.7.4), using 5 μm intervals. Dendrite intersections (i.e., branching) and maximum dendrite length were characterized by this Sholl analysis. For each group, 3–4 pyramidal CA1 neurons per brain from 4 mice per group were analyzed, under blinded conditions.

Dendritic spine density, calculated as the number of spines (i.e., small protrusions) per segment normalized to the length of the segment, was assessed using 3rd branch order dendritic branches at 100x magnification. For each treatment group, spine density was measured in 3 pyramidal CA1 neurons (two third order branches per neuron) per mouse from 4 mice, under blinded conditions.

2.9. Cell culture

Murine microglial cells (BV2, ATCC CRL-2469) and murine macrophages (RAW 264.7, ATCC TIB-71) were grown in DMEM (Gibco, low glucose or high glucose, respectively) supplemented with 10% (v/v) FBS and 1% (v/v) Penicillin-Streptomycin (Pen-Strep; 10.000 U/ml; Gibco). Human monocytes (THP-1, ATCC TIB-202) were cultured in RPMI supplemented with 10% FBS, 1% Pen-Strep and 50 μM 2-mercaptoethanol until 80% confluency. THP-1 cells were differentiated using phorbol-12-myristate-13-acetate (PMA; 100 ng/ml) for 24 h; and thereafter rested for 3 days to allow for differentiation. All cell types were incubated with vehicle or lipopolysaccharide (LPS; 100 ng/ml) for 24 h and simultaneously subjected to CFTR modulators ivacaftor (+ Iva), lumacaftor (+ Lum) or vehicle control (Ctrl).

2.10. Quantitative real-time PCR

Total RNA was extracted from BV2, RAW264.7 and THP-1 cells using TriZol Reagent (Invitrogen) according to manufacturer's instructions. 500 ng of total RNA was reverse transcribed with random hexamer primers using a "High-Capacity Reverse Transcriptase Kit" kit (Applied Biosystems; Gothenburg, Sweden). cDNA was diluted with RNAse-free water (1:12.5) and used as template for quantitative real-time PCR (qRT-PCR) reactions. Gene expression was determined with qRT-PCR, using Fast SYBR Green (Applied Biosystems, Naerum, Denmark) and 0.2 μM gene specific forward and reverse primers (Supplemental Table 2) in a CFX384 TouchTM Real-Time PCR Detection System (Bio-Rad; Sundbyberg, Sweden) with the cycling parameters: 95 °C for 10 min, a total of 39 cycles (95 °C for 15 s, 60 °C for 1 min) followed by a dissociation stage (95 °C for 1 min, 55 °C for 70 s and 95 °C for 50 s). Data were analyzed using standard curves generated from a pooled cDNA sample to be analyzed and normalized to the housekeeping genes.

2.11. Statistics

Using previous data as guidance [19,28,31,32], the experimental group sizes necessary to ensure that all data provide a power of 80% power ($1\text{-}\beta > 0.8$) and a two-tailed Type I alpha error of 0.05 were calculated.

All assessments and analyses in the current study were performed under blinded conditions, using codes that concealed the identity of the intervention. Data were analyzed using GraphPad Prism 9 software (San Diego, California). Normality of the data was determined by the Shapiro-Wilk test. Normally distributed data are presented as mean ± standard error of the mean (SEM) and compared using parametric statistical tests. Data that are not normally distributed are presented as median ± interquartile range (IQR) and are compared using non-parametric statistical tests. Student's t-tests or Mann Whitney tests are used to compare two independent groups; one-way analysis of variance (ANOVA) with Dunnett *post-hoc* test or Kruskal Wallis test with Dunn's *post-hoc* test are used to compare multiple independent groups. Differences are regarded as significant at $p \leq 0.05$. For all data sets, N represents the number of animals or independent biological sample and n the number of independent measures. All figure data, sample size, and statistical test outcomes are presented in Supplemental Table 3 & 4.

2.12. Role of the funding sources

The study sponsors did not play any role in study design; collection, analysis, and interpretation of the data; manuscript preparation; nor the decision to submit for publication.

3. Results

3.1. Ivacaftor therapy attenuates post-MI brain alterations

In previous studies, we showed that increasing CFTR expression using C18, lumacaftor and lumacaftor/ivacaftor therapies improved MI-associated neurodegeneration with implication for memory function [19,20]. Here, we test whether CFTR potentiation using ivacaftor as monotherapy accommodates similar beneficial effects in MI-associated brain alterations.

Two weeks of ivacaftor therapy (1.875 mg/kg by daily i.p. injection) mitigates MI-associated dendritic atrophy of CA1 hippocampal pyramidal neurons (Fig. 1A-C) evidenced by significantly longer dendrites (Fig. 1B-C) and higher spine density (Fig. 1D) compared to vehicle-treated MI mice. A direct comparison between ivacaftor effects and previously published data on lumacaftor effects on dendrite spine density post-MI [20] reveals a lower drug-to-vehicle ratio in the ivacaftor study (1.1 vs. 1.6; Supplemental Fig. 1). Despite the potentially lower efficacy of attenuating alterations in neuronal structures, ivacaftor monotherapy substantially improves MI-associated hippocampus-dependent memory impairment (Fig. 1E).

3.2. Ivacaftor therapy post-MI leads to increased systemic inflammation

Previously published results suggested an attenuation of MI-associated immune system activation by therapeutic administration of the CFTR corrector C18 [19]. Ivacaftor monotherapy augments frequencies of several circulating myeloid cell populations, including $Ly6C^{+}$ cells, pro-inflammatory monocytes ($Ly6C^{hi}$) and neutrophils (Table 1), indicating a systemic activation of the immune system. In contrast to ivacaftor, lumacaftor therapy does not alter frequencies of these immune cell subsets (Table 1), suggesting CFTR modulator-specific systemic immune responses.

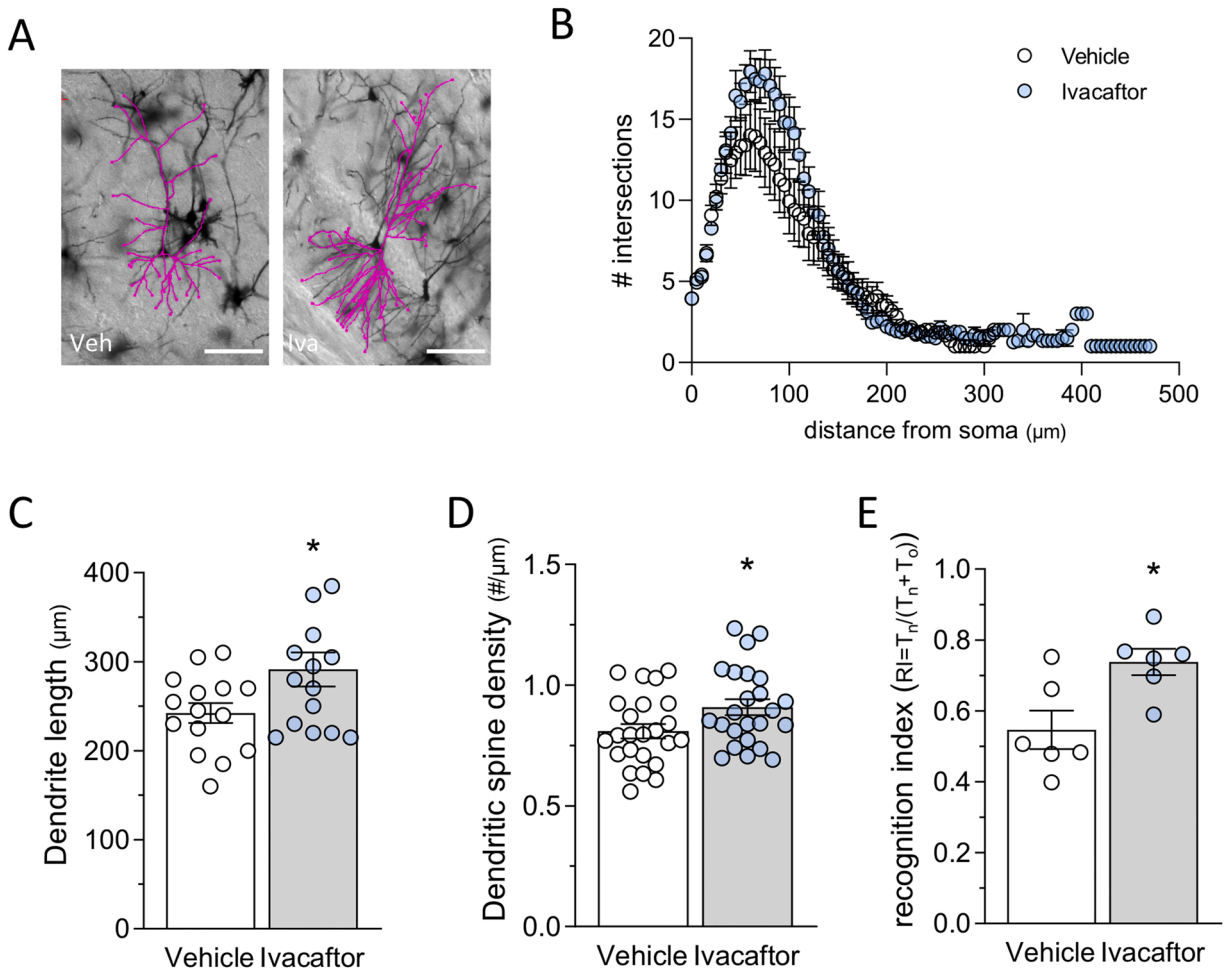

Fig. 1. Ivacaftor is protective for MI-induced neurodegeneration and cognitive impairment. (A) Shown are representatives of Golgi Cox-stained pyramidal, hippocampal cornu ammonis (CA1) neurons from vehicle or ivacaftor treated mice at 12 weeks post-myocardial infarction (MI). The dendrite's arborization is highlighted with traces superimposed onto the images. Ivacaftor therapy (Iva; 1.875 mg/kg daily for 2 weeks, starting at 10 weeks post-MI) does not significantly influence (B) the number of intersections of CA1 pyramidal neurons (n = 3–4 neurons from N = 4 mice), however effectively increases (C) mean dendrite length (n = 3–4 neurons from N = 4 mice), (D) pyramidal CA1 neuron dendrite spine density (n = 24 analyzed branches from N = 4 mice) in the hippocampus; and (E) Iva normalizes hippocampal-dependent retention of object familiarity in a non-spatial novel object recognition task (N = 6; 2 mice from MI + vehicle and 2 mice from MI + Lum/Iva groups were excluded due to total exploration times below 20 s). * denotes $p < 0.05$ for unpaired comparisons. *Panels C, D and E* are presented as mean ± SEM and are compared with Student's t-test. Bar over micrographs is 100 μm in Panel A.

3.3. MI-associated pulmonary inflammation but not neuroinflammation is exacerbated after ivacaftor therapy

Therapeutic augmentation of CFTR cell surface expression, specifically on non-alveolar macrophages, using lumacaftor attenuates tissue-specific inflammation in the lung post-MI by mitigating adverse macrophage polarization [22]. Expectedly, CFTR surface expression of pulmonary cells, including non-alveolar macrophages ($F4/80^+$ $SiglecF^-$ cells) is unchanged after ivacaftor potentiator treatment (i.e., ivacaftor does not attenuate MI-induced CFTR downregulation; Supplemental Fig. 2). In accordance, macrophage phenotype profiling reveals increased frequencies of $CD80^+$ $F4/80^+$ as well as $F4/80^+$ non-alveolar and alveolar ($F4/80^+$ $SiglecF^+$) cells in the ivacaftor group (Table 2a-c), indicative of a proinflammatory phenotype. When comparing to previously published data on lumacaftor effects [22], the $CD80^+$ cell ratio of drug-to-vehicle is higher after ivacaftor compared to lumacaftor monotherapy (2 vs. 1.4 for all subsets; Supplemental Fig. 3A), suggesting that improper CFTR cell surface expression contributes to the observed pro-inflammatory ivacaftor effects in the lung post-MI. In contrast to results obtained after lumacaftor treatment [22], frequencies of all $CD206^+$ $F4/80^+$ as well as non-alveolar and alveolar $CD206^+$ $F4/80^+$cells remain largely unaffected by ivacaftor treatment (Table 2d-f). Thus, drug-to-vehicle ratios of $CD206^+$ cells are lower with ivacaftor compared to lumacaftor treatment (2 vs. 4 for all subsets; Supplemental Fig. 3B).

Contrasting the findings in the lung, MI-associated activation of brain-specific macrophages (i.e., microglia; [20,28]) is attenuated by ivacaftor monotherapy. Morphological assessment of microglial cells in hippocampus regions (CA1 and DG) reveals significantly lower proportions of intermediate and round (i.e., activated) microglia, while percentages of ramified, resting phenotype are higher in ivacaftor compared to vehicle-treated MI mice (Fig. 2A-B).

3.4. Ivacaftor evokes cell-type dependent effects in vitro

Results obtained in in vitro experiments utilizing different macrophage cell types suggest a cell type-specific inflammatory potential of ivacaftor. Specifically, ivacaftor leads to an augmentation of LPS-induced CD80 and TNF-α mRNA expression in human monocyte-derived macrophages (Fig. 3A; Supplemental Fig. 4 A) and murine macrophages (Fig. 3B; Supplemental Fig. 4B). This contrasts its effects in BV2 microglial cells where ivacaftor does not augment LPS-induced CD80 and TNF-α mRNA expression (Fig. 3C, Supplemental Fig. 4C). Treatment with lumacaftor, on the other hand, does not affect CD80 nor

Table 1
Ivacaftor, but not lumacaftor, augments systemic inflammation post-MI.

	Cell type (#)	Veh	Iva	p-value
a	**B-cells**	125,075 ± 13,689	133,756 ± 9,881	p = 0.62
b	**T-cells**	28,009 ± 5,051	39,890 ± 3,606	p = 0.08
c	**Ly6C^{+}**	15,310 ± 1,343	23,343 ± 3,077	**p = 0.04**
d	**Ly6C^{hi}**	7,194 ± 692	11,501 ± 1,654	**p = 0.04**
e	**Neutrophils**	18,077 ± 2,811	34,158 ± 5,057	**p = 0.01**
	Cell type (#)	Veh	Lum	p-value
f	**B-cells**	87,699 ± 11,267	100,946 ± 12,153	p = 0.45
g	**T-cells**	38,702 ± 4,113	47,600 ± 4,598	p = 0.18
h	**Ly6C^{+}**	15,778 ± 2,454	16,877 ± 2,408	p = 0.76
i	**Ly6C^{hi}**	6,009 ± 897	5,900 ± 910	p = 0.93
j	**Neutrophils**	23,445 ± 12,341	26,939 ± 15,060	p = 0.50

Ten weeks post myocardial infarction, mice were administered vehicle or CFTR modulator treatment daily for 2 consecutive weeks. Two cohorts are used each containing one vehicle group and a treatment group that received different CFTR modulators: (i) ivacaftor (Iva; 1.875 mg/kg) or (ii) lumacaftor (Lum; 3mg/kg). Iva administration (a-e) further increases the number of circulating immune cells compared to their vehicle control, while (f-j) Lum does not alter circulating immune cell levels, compared to their vehicle control group. P-values for unpaired comparisons are indicated, with significant differences marked in red. Rows a, b, c d, f, g, h, i and j are presented as mean ± SEM and are compared with Student's t-test; Row e, is presented as median ± IQR and compared with Mann-Whitney.

Table 2
Ivacaftor increases frequencies of pro-inflammatory pulmonary macrophage subsets.

	Macrophage type (#)	Veh	Iva	p-value
a	**All (CD80^{+} F4/80^{+})**	4,116 ± 1,134	8,745 ± 5,727	**p = 0.0148**
b	**non-alveolar (CD80^{+} SiglecF^{-} F4/80^{+})**	3,336 ± 1,212	6,807 ± 5,158	**p = 0.0281**
c	**alveolar (CD80^{+} SiglecF^{+} F4/80^{+})**	847 ± 154	1,602 ± 269	**p = 0.0290**
d	**All (CD206^{+} F4/80^{+})**	3,177 ± 2,035	5,370 ± 5,466	p = 0.1949
e	**non-alveolar (CD206^{+} SiglecF^{-} F4/80^{+})**	2,904 ± 1,453	4,611 ± 4,739	p = 0.1949
f	**alveolar (CD206^{+} SiglecF^{+} F4/80^{+})**	434 ± 858	899 ± 943	p = 0.3824

Ivacaftor (1.875 mg/kg daily for 2 weeks, starting at 10 weeks post-MI) treatment results in increased CD80-positivity in all (**a**; CD80^{+} F4/80^{+}), non-alveolar (**b**; CD80^{+} SiglecF^{-} F4/80^{+}), and alveolar cells (**c**; CD80^{+} SiglecF^{+} F4/80^{+}), while not changing CD206-expressing cells (**d-f**). P-values for unpaired comparisons are indicated, with significant differences marked in red. *Rows a, b, d, e, f* are presented as median ± IQR and are compared with Mann-Whitney; *Row c* is presented as mean ± SEM and are compared with Student's t-test.

TNF-α mRNA expression (Fig. 3A, B, C; Supplemental Fig. 4A, B, C) with the exception TNF-α that is increased in response to lumacaftor in human monocyte-derived macrophages (Supplemental Fig. 4A). In BV2 microglial cells, lumacaftor decreases TNF-α mRNA expression (Supplemental Fig. 4C).

Importantly, ivacaftor increases CD80 and TNF-α expression in the absence of LPS in human macrophages, while lumacaftor has no such effects (Fig. 3D; Supplemental Fig. 4D). In murine macrophages and BV2 microglial cells and, CD80 (Fig. 3E, F) and TNF-α (Supplemental Fig. 4E, F) expression are not affected by either ivacaftor or lumacaftor treatment in the absence of LPS. Together, this data suggests macrophage type-specific ivacaftor effects.

4. Discussion

This investigation demonstrates that treatment with the CFTR potentiator ivacaftor evokes contrasting effects in different target tissues post-MI. In the brain, systemic ivacaftor therapy mitigates MI-associated dendrite atrophy of hippocampal pyramidal neurons as well as hippocampal memory impairment and attenuates adverse microglia activation induced by MI. In contrast, systemic ivacaftor therapy enhances peripheral immune system activation and induces a pro-inflammatory macrophage profile in the post-MI lung. *In vitro* experiments confirm cell type-specific ivacaftor effects with respect to its inflammatory potential, which may be the cause of both beneficial and adverse tissue-dependent effects evoked by systemic ivacaftor therapy.

CFTR potentiator compounds like ivacaftor increase the activity of dysfunctional CFTR at the cell surface, whereas corrector compounds improve defective protein processing and trafficking to the cell surface. Furthermore, CFTR potentiators enhance the function of wild type forms of CFTR [33–35], enabling new therapeutic strategies for the treatment of acquired CFTR dysfunction associated with several diseases. An initial evaluation of ivacaftor therapy in COPD patients with chronic bronchitis yielded promising, yet non-significant improvements in CFTR function accompanied by minor symptom relieve [2]. The study, however, was underpowered and warrants a larger trial allowing for better associations of CFTR activity with lung function parameters. In a separate study, ivacaftor was shown to reverse acquired CFTR abnormalities resulting from cigarette smoke exposure, such as reduced CFTR-mediated anion secretion that rapidly inhibited ciliary beating function of airway monolayers in vitro [36], suggesting beneficial ivacaftor effects when treating acquired CFTR dysfunction in the lung.

Although the observed effects of ivacaftor on lung function seem promising, inflammation has rarely been investigated in these studies despite its obvious role in diseases such as CF, COPD, and chronic bronchitis [37,38]. In CF, contradictive results from the limited number of available studies that focus on sputum inflammation markers hinder clear conclusions regarding ivacaftor's effects [39,40]. Moreover, studying sputum inflammatory markers does not reflect systemic inflammation, which would be interesting to study considering the generally systemic administration route of ivacaftor. Particularly, systemic administration and lipophilic properties that make both ivacaftor and lumacaftor permeable to the blood-brain barrier [41], necessitate the investigation of their effects systemically (i.e., in the whole body). In diseases where solely the lung is affected by acquired CFTR downregulation, the possibility for direct pulmonary drug application could be an interesting approach to avoid possible systemic side effects. We have previously studied different administration routes of the CFTR modulator lumacaftor (i.e., i.p. and oro-tracheal (o.t.)), where local (o.t.) treatment shows a more efficient increase in CFTR expression and has similar effects on the phenotype of alveolar and non-alveolar macrophages compared to systemically (i.p.) treated mice [22]. Nonetheless, we have also noted an administration-specific activation of lung-resident macrophages after o.t. treatment, potentially limiting its beneficial effects long-term. Recently, the use of spray dried inhalable ivacaftor has been suggested as a potential approach for pulmonary administration of hydrophobic drugs [42]. However, when CFTR function is affected in multiple organs, such as after MI, systemic drug administration will likely remain the first-line therapy. In lung diseases such as COPD and chronic bronchitis, it is thus far unknown whether CFTR downregulation is isolated to the lung or also affects other organs. Evidently, more research regarding target organ effects and different administration routes is necessary to enable safe and efficacious repurposing of CFTR modulators for diseases other than CF.

In the current study, systemic ivacaftor treatment post-MI associates with increased systemic and pulmonary inflammation extending beyond that of vehicle-treated mice. In contrast to the lung, this augmented systemic inflammation does not show detrimental effects on the brain as systemic ivacaftor therapy attenuates MI-associated neuroinflammation in the hippocampus, which correlates with improvements in hippocampal neuronal structure and memory function. Specifically, cells of the myeloid lineage seem to respond differently to systemic ivacaftor treatment. With respect to CFTR function in myeloid cells it was shown

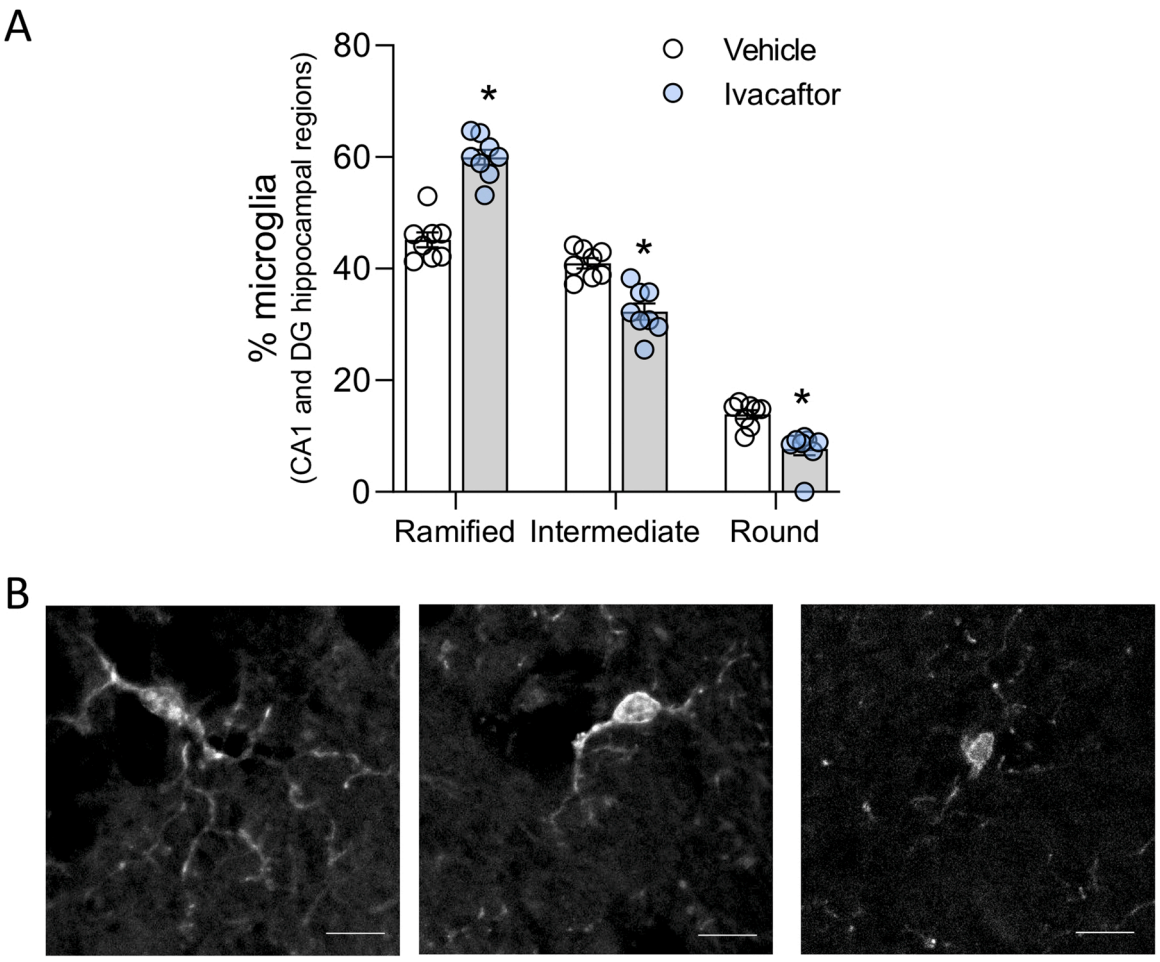

Fig. 2. Ivacaftor reduces microglial activation. (A) Ivacaftor (1.875 mg/kg daily for 2 weeks, starting at 10 weeks post myocardial infarction) effectively reduces microglia activation as apparent by increased percentage of ramified (resting) microglia and decreases in the intermediate and round (active) phenotype in cornu ammonis 1 (CA1) and dentate gyrus (DG) hippocampal regions. (B) Representative images of ramified, intermediate and active microglia. * denotes $p < 0.05$ for unpaired comparisons. All groups are presented as mean ± SEM. *Ramified and intermediate* are compared with Student's t-test; *round* is compared with Mann-Whitney. Bar in the micrographs is 10 μm.

that monocyte derived macrophages (MDM) from CF patients present with a 2-fold higher apoptotic rate compared to non-CF MDMs [43]. In CFTR-deficient mice, myeloid cells such as alveolar and bone-marrow derived macrophages (BMDM) present with elevated levels of inflammatory cytokines after in vitro LPS stimulation compared to WT cells [44]. Interestingly, the same study confirms these findings in vivo by transplantation of WT BMDM into $CFTR^{-/-}$ mice, which corrects a significant fraction of LPS-induced inflammation in $CFTR^{-/-}$ mice [44]. Another group investigated ivacaftor effects in combination with o.t. LPS administration and showed that preventative ivacaftor administration leads to an increased macrophage infiltration compared to control, which is suggestive of a potential priming of the lung towards an inflammatory response [45]. This ivacaftor effect may be independent of its CFTR corrector function, however, pharmacochemical studies are needed to mechanistically underpin this. The currently only longitudinal study to characterize ivacaftor effects on systemic inflammation and the blood proteome in CF patients showed increases in several regulators of inflammation [46], including repulsive guidance molecule A (RGMA) that has been show to activate T-cells and promote pathogenic T-helper 17 responses [47] and afamin, which has been associated with plasma inflammation markers such as c-reactive protein in metabolic syndrome [48]. Similar increases of pituitary adenylate cyclase-activating polypeptide (PACAP-38) after ivacaftor [46] are indicative of its immunomodulatory effects as PACAP-38 protects $CD4^{+}$ T-cells from activation induced cell death [49] and differentially affects macrophages towards pro- or anti-inflammatory pathways [50]. Whether these regulators of inflammation are directly modulated by ivacaftor or result from indirect drug effects remains to be determined. It will furthermore be important to investigate whether CFTR potentiation alone is sufficient to compensate for the absence of CFTR, which has been associated with inflammation in multiple cell types. Studies reported that CFTR deficiency can trigger inflammation in neutrophils and platelets [51], the absence of CFTR in myeloid cells slows down resolution of infection and inflammation [52], and CFTR has been shown to play a role in proper lysosomal acidification [53]. We have previously shown that down-regulation of CFTR correlates with an enhanced pro-inflammatory immune cell profile in the lung post-MI. Cigarette smoke has been found to reduce CFTR expression and function [17] which is related to impaired bacterial phagocytosis [53,54], favoring recurrent infections and airway inflammation [55]. Whether CFTR is affected on myeloid cells in vivo during COPD and chronic bronchitis is yet to be determined.

Other CFTR modulators may also be of interest for repurposing. One of the most widely used CFTR corrector compounds, lumacaftor, has not been clinically approved as a monotherapy, hence little is known about its effects in the absence of ivacaftor. In CF, combination therapy of lumacaftor with ivacaftor often shows beneficial effects (e.g., increased FEV1, reduced hospitalizations due to pulmonary exacerbations) [56,57]. However, effects of combination therapy in diseases with acquired CFTR deficiencies are rarely investigated. Some studies suggest that ivacaftor can diminish beneficial effects of lumacaftor; for example,

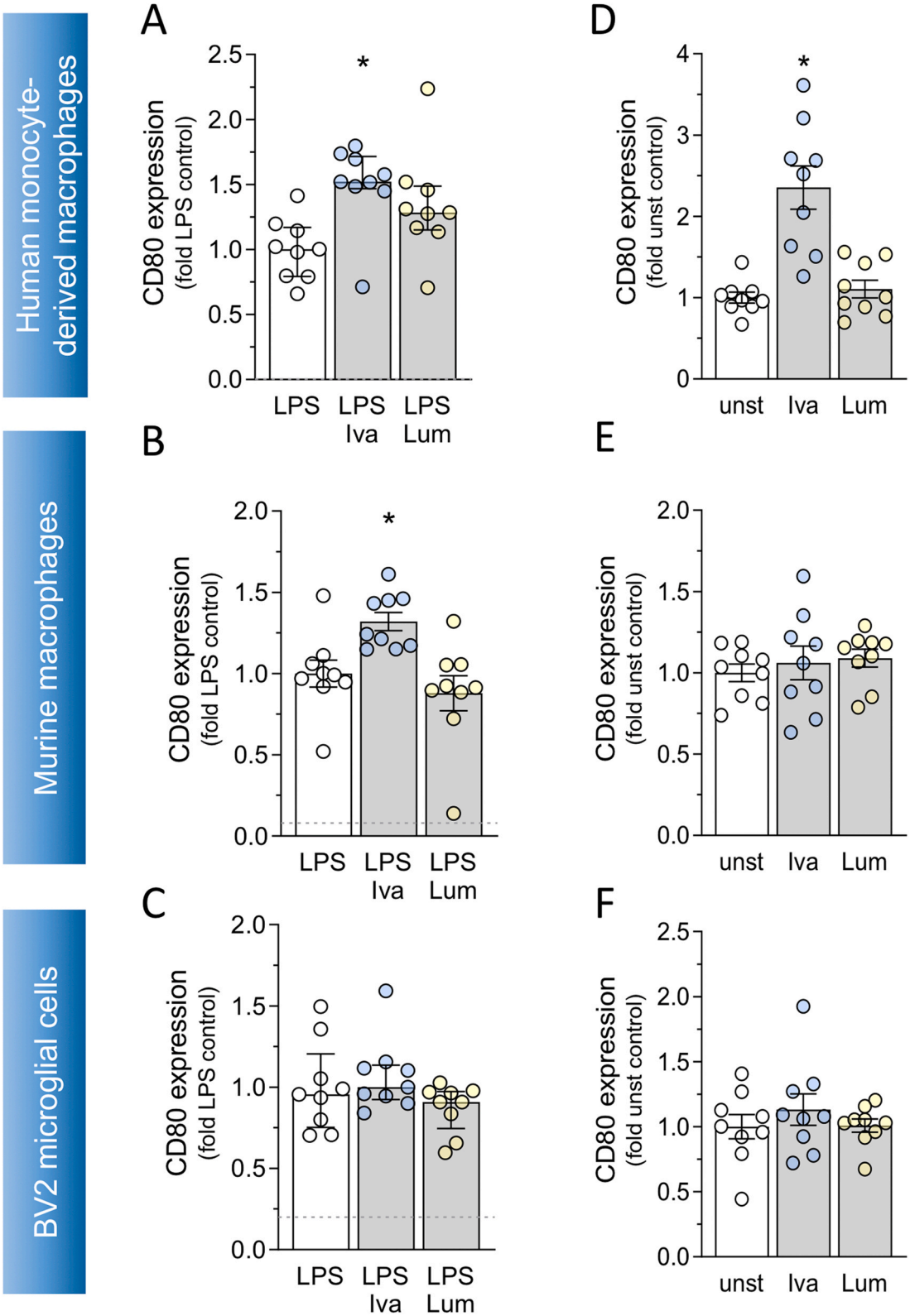

Fig. 3. Ivacaftor exacerbates LPS-induced inflammation in human and murine macrophages, but not microglia in vitro. Lipopolysaccharide (LPS; 100 ng/ml, for 24 h) augmented CD80 mRNA expression in differentiated human monocyte-derived macrophages (THP-1 cells), murine RAW264.7, and BV2 microglial cells. Dotted lines in the graphs indicate control levels. Simultaneous application of ivacaftor (Iva, 10 μM), but not lumacaftor (Lum, 10 μM) augments the LPS response in (A) differentiated human monocyte-derived macrophages or (B) murine RAW264.7 cells. (C) Neither simultaneous ivacaftor (Iva, 10 μM) nor lumacaftor treatment (Lum, 10 μM) increase the LPS response in murine BV2 microglial cells. In absence of LPS, ivacaftor treatment stimulates CD80 mRNA expression in (D) human, but not (E) murine macrophages or (F) BV2 microglial cells. * denotes $p < 0.05$ for unpaired comparisons. *Panels B, D, E and F* are presented as mean ± SEM and are compared with ANOVA followed by Dunnett́s post-hoc testing. *Panels A and C* are presented as median ± IQR and are compared with Kruskal-Wallis followed by Dunńs post-hoc testing.

ivacaftor reduced lumacaftor-stimulated phagocytosis of *Pseudomonas aeruginosa* in CF MDMs [58]. Although, as CF macrophages are intrinsically hyperinflammatory, the observed effects of CFTR modulators cannot be generalized [59]. Cells in diseases with acquired CFTR deficiency do not bear genetic CFTR defects, hence different effects might occur. Considering the different pathophysiology of CFTR defects in other diseases, a monotherapy of one CFTR modulator may be favored over a combination treatment such as Orkambi® (lumacaftor/-ivacaftor). Interestingly, until today lumacaftor monotherapy has not been assessed in clinical trials at the dose in which it is currently used in the combination treatment regimen for CF.

Repurposing CFTR modulator compounds for diseases other than CF represent a promising new therapeutic approach. The herein presented results of ivacaftor therapy post-MI call for caution due to proinflammatory effects, but also show the therapeutic potential with regard to positive effects in the brain. In future studies, it will be important to investigate both the CFTR-modulating functional outcome in the respective target organ and the effects on inflammation, locally as well as systemically.

Funding

This study was financially supported by: The Knut and Alice Wallenberg Foundation [F 2015/2112; A.M.]; Hjärnfonden [FO2021-0112; A.M.]; Crafoord Foundation [20220654; A.M., 20190782; F.E.U.]; NMMP 2021 [V2021–2102; A.M.]; the Albert Påhlsson Research Foundation [120482; A.M.]; Royal Physiographic Society of Lund [43037; L. V.]; STINT [MG19-8469; A.M.], Lund University [A.M.] and University of Augsburg [A.M., F.M.].

CRediT authorship contribution statement

Conceptualization, A.M.; Methodology, L.V., F.M., F.E.U., and A.M.; Validation, L.V., F.M., and A.M.; Formal analysis, L.V., F.M., F.E.U., and A.M.; Data curation, L.V., F.M., F.E.U., and A.M.; verified the underlying data, L.V., and A.M.; Writing – original draft preparation, L.V., and A.M.; Writing – conceptual review and editing, L.V., F.M., and A.M.; Visualization, L.V., F.M. and A.M.; Supervision, A.M.; Project administration, A.M.; Funding acquisition, L.V., F.M., F.E.U., and A.M.; decision to submit the manuscript, L.V., and A.M. All authors have read and agreed to the published version of the manuscript.

Declaration of Competing Interest

The authors declare that they have no known competing financial interests or personal relationships that could have appeared to influence the work reported in this paper.

Acknowledgements

The authors thank the Lund University BioImaging Center (LBIC) for access to the Nikon Ti2 Eclipse microscope.

Appendix A. Supporting information

Supplementary data associated with this article can be found in the online version at doi:10.1016/j.biopha.2023.114628.

References

[1] B. Kerem, J.M. Rommens, J.A. Buchanan, D. Markiewicz, T.K. Cox, A. Chakravarti, M. Buchwald, L.C. Tsui, Identification of the cystic fibrosis gene: genetic analysis, Science 245 (4922) (1989) 1073–1080.
[2] G.M. Solomon, H. Hathorne, B. Liu, S.V. Raju, G. Reeves, E.P. Acosta, M. T. Dransfield, S.M. Rowe, Pilot evaluation of ivacaftor for chronic bronchitis, Lancet Respir. Med 4 (6) (2016) e32–e33.
[3] G.M. Solomon, L. Fu, S.M. Rowe, J.F. Collawn, The therapeutic potential of CFTR modulators for COPD and other airway diseases, Curr. Opin. Pharm. 34 (2017) 132–139.
[4] L. Carrasco-Hernández, E. Quintana-Gallego, C. Calero, R. Reinoso-Arija, B. Ruiz-Duque, J.L. López-Campos, Dysfunction in the cystic fibrosis transmembrane regulator in chronic obstructive pulmonary disease as a potential target for personalised medicine, Biomedicines 9 (10) (2021).
[5] M. Wilschanski, I. Novak, The cystic fibrosis of exocrine pancreas, Cold Spring Harb. Perspect. Med 3 (5) (2013) a009746.
[6] A. Meissner, J. Yang, J.T. Kroetsch, M. Sauvé, H. Dax, A. Momen, M.H. Noyan-Ashraf, S. Heximer, M. Husain, D. Lidington, S.S. Bolz, Tumor necrosis factor-α-mediated downregulation of the cystic fibrosis transmembrane conductance regulator drives pathological sphingosine-1-phosphate signaling in a mouse model of heart failure, Circulation 125 (22) (2012), 2739-50.
[7] Y. Guo, M. Su, M.A. McNutt, J. Gu, Expression and distribution of cystic fibrosis transmembrane conductance regulator in neurons of the human brain, J. Histochem Cytochem 57 (12) (2009), 1113-20.
[8] M.M. Morales, T.P. Carroll, T. Morita, E.M. Schwiebert, O. Devuyst, P.D. Wilson, A. G. Lopes, B.A. Stanton, H.C. Dietz, G.R. Cutting, W.B. Guggino, Both the wild type and a functional isoform of CFTR are expressed in kidney, Am. J. Physiol. 270 (6 Pt 2) (1996). F1038-48.
[9] N.S. Alexander, A. Blount, S. Zhang, D. Skinner, S.B. Hicks, M. Chestnut, F. A. Kebbel, E.J. Sorscher, B.A. Woodworth, Cystic fibrosis transmembrane conductance regulator modulation by the tobacco smoke toxin acrolein, Laryngoscope 122 (6) (2012), 1193-7.
[10] C. Azbell, S. Zhang, D. Skinner, J. Fortenberry, E.J. Sorscher, B.A. Woodworth, Hesperidin stimulates cystic fibrosis transmembrane conductance regulator-mediated chloride secretion and ciliary beat frequency in sinonasal epithelium, Otolaryngol. Head. Neck Surg. 143 (3) (2010) 397–404.
[11] X. Wang, J. Kim, R. McWilliams, G.R. Cutting, Increased prevalence of chronic rhinosinusitis in carriers of a cystic fibrosis mutation, Arch. Otolaryngol. Neck Surg. 131 (3) (2005) 237–240.
[12] L.A. Clunes, C.M. Davies, R.D. Coakley, A.A. Aleksandrov, A.G. Henderson, K. L. Zeman, E.N. Worthington, M. Gentzsch, S.M. Kreda, D. Cholon, W.D. Bennett, J. R. Riordan, R.C. Boucher, R. Tarran, Cigarette smoke exposure induces CFTR internalization and insolubility, leading to airway surface liquid dehydration, FASEB J. 26 (2) (2012), 533-45.
[13] J.D. Londino, A. Lazrak, J.W. Noah, S. Aggarwal, V. Bali, B.A. Woodworth, Z. Bebok, S. Matalon, Influenza virus M2 targets cystic fibrosis transmembrane conductance regulator for lysosomal degradation during viral infection, FASEB J. 29 (7) (2015), 2712-25.
[14] S.V. Raju, G.M. Solomon, M.T. Dransfield, S.M. Rowe, Acquired cystic fibrosis transmembrane conductance regulator dysfunction in chronic bronchitis and other diseases of mucus clearance, Clin. Chest Med 37 (1) (2016), 147-58.
[15] J.M. Bomberger, S. Ye, D.P. Maceachran, K. Koeppen, R.L. Barnaby, G.A. O'Toole, B.A. Stanton, A Pseudomonas aeruginosa toxin that hijacks the host ubiquitin proteolytic system, PLoS Pathog. 7 (3) (2011), e1001325.
[16] J.E. Rasmussen, J.T. Sheridan, W. Polk, C.M. Davies, R. Tarran, Cigarette smoke-induced Ca2+ release leads to cystic fibrosis transmembrane conductance regulator (CFTR) dysfunction, J. Biol. Chem. 289 (11) (2014), 7671-81.
[17] A.M. Cantin, J.W. Hanrahan, G. Bilodeau, L. Ellis, A. Dupuis, J. Liao, J. Zielenski, P. Durie, Cystic fibrosis transmembrane conductance regulator function is suppressed in cigarette smokers, Am. J. Respir. Crit. Care Med 173 (10) (2006), 1139-44.
[18] A. Rab, S.M. Rowe, S.V. Raju, Z. Bebok, S. Matalon, J.F. Collawn, Cigarette smoke and CFTR: implications in the pathogenesis of COPD, Am. J. Physiol. Lung Cell Mol. Physiol. 305 (8) (2013). L530-41.
[19] D. Lidington, J.C. Fares, F.E. Uhl, D.D. Dinh, J.T. Kroetsch, M. Sauve, F.A. Malik, F. Matthes, L. Vanherle, A. Adel, A. Momen, H. Zhang, R. Aschar-Sobbi, W.D. Foltz, H. Wan, M. Sumiyoshi, R.L. Macdonald, M. Husain, P.H. Backx, S.P. Heximer, A. Meissner, S.S. Bolz, CFTR therapeutics normalize cerebral perfusion deficits in mouse models of heart failure and subarachnoid hemorrhage, JACC Basic Transl. Sci. 4 (8) (2019) 940–958.
[20] L. Vanherle, D. Lidington, F.E. Uhl, S. Steiner, S. Vassallo, C. Skoug, J.M.N. Duarte, S. Ramu, L. Uller, J.-F. Desjardins, K.A. Connelly, S.-S. Bolz, A. Meissner, Restoring myocardial infarction-induced long-term memory impairment by targeting the cystic fibrosis transmembrane regulator, eBioMedicine 86 (2022), 104384.
[21] F.E. Uhl, L. Vanherle, F. Matthes, A. Meissner, Therapeutic CFTR correction normalizes systemic and lung-specific S1P level alterations associated with heart failure, Int. J. Mol. Sci. 23 (2) (2022) 866.
[22] F.E. Uhl, L. Vanherle, A. Meissner, Cystic fibrosis transmembrane regulator correction attenuates heart failure-induced lung inflammation, Front Immunol. 13 (2022), 928300.
[23] H. Fischer, The G551D CFTR chloride channel spurs the development of personalized medicine, J. Physiol. 592 (9) (2014), 1907-8.
[24] A. Hollis, Orphan drug pricing and costs: a case study of kalydeco and orkambi, Health Policy 15 (1) (2019) 70–80.
[25] H.N. Ásgeirsdóttir, S.J. Cohen, R.W.S. Jr., Object and place information processing by CA1 hippocampal neurons of C57BL/6J mice, Journal of Neurophysiology 123 (3) (2020) 1247–1264.
[26] S.J. Cohen, A.H. Munchow, L.M. Rios, G. Zhang, H.N. Asgeirsdóttir, R. W. Stackman Jr., The rodent hippocampus is essential for nonspatial object memory, Curr. Biol. 23 (17) (2013), 1685-90.
[27] N. Don-Doncow, L. Vanherle, F. Matthes, S.K. Petersen, H. Matuskova, S. Rattik, A. Hartlova, A. Meissner, Simvastatin therapy attenuates memory deficits that

associate with brain monocyte infiltration in chronic hypercholesterolemia, NPJ Aging Mech. Dis. 7 (1) (2021) 19.
[28] A. Meissner, N.P. Visanji, M.A. Momen, R. Feng, B.M. Francis, S.S. Bolz, L. N. Hazrati, Tumor necrosis factor-alpha underlies loss of cortical dendritic spine density in a mouse model of congestive heart failure, J. Am. Heart Assoc. 4 (5) (2015).
[29] S. Zaqout, A.M. Kaindl, Golgi-cox staining step by step, Front Neuroanat. 10 (2016) 38.
[30] D.A. Sholl, Dendritic organization in the neurons of the visual and motor cortices of the cat, J. Anat. 87 (4) (1953) 387–406.
[31] A. Meissner, J. Yang, J.T. Kroetsch, M. Sauve, H. Dax, A. Momen, M.H. Noyan-Ashraf, S. Heximer, M. Husain, D. Lidington, S.S. Bolz, Tumor necrosis factor-alpha-mediated downregulation of the cystic fibrosis transmembrane conductance regulator drives pathological sphingosine-1-phosphate signaling in a mouse model of heart failure, Circulation 125 (22) (2012), 2739-50.
[32] J. Yang, M.H. Noyan-Ashraf, A. Meissner, J. Voigtlaender-Bolz, J.T. Kroetsch, W. Foltz, D. Jaffray, A. Kapoor, A. Momen, S.P. Heximer, H. Zhang, M. van Eede, R. M. Henkelman, S.G. Matthews, D. Lidington, M. Husain, S.S. Bolz, Proximal cerebral arteries develop myogenic responsiveness in heart failure via tumor necrosis factor-alpha-dependent activation of sphingosine-1-phosphate signaling, Circulation 126 (2) (2012) 196–206.
[33] F. Van Goor, S. Hadida, P.D. Grootenhuis, B. Burton, D. Cao, T. Neuberger, A. Turnbull, A. Singh, J. Joubran, A. Hazlewood, J. Zhou, J. McCartney, V. Arumugam, C. Decker, J. Yang, C. Young, E.R. Olson, J.J. Wine, R.A. Frizzell, M. Ashlock, P. Negulescu, Rescue of CF airway epithelial cell function in vitro by a CFTR potentiator, VX-770, Proc. Natl. Acad. Sci. USA 106 (44) (2009), 18825-30.
[34] P.A. Sloane, S. Shastry, A. Wilhelm, C. Courville, L.P. Tang, K. Backer, E. Levin, S. V. Raju, Y. Li, M. Mazur, S. Byan-Parker, W. Grizzle, E.J. Sorscher, M.T. Dransfield, S.M. Rowe, A pharmacologic approach to acquired cystic fibrosis transmembrane conductance regulator dysfunction in smoking related lung disease, PLoS One 7 (6) (2012), e39809.
[35] N. Pedemonte, V. Tomati, E. Sondo, L.J. Galietta, Influence of cell background on pharmacological rescue of mutant CFTR, Am. J. Physiol. Cell Physiol. 298 (4) (2010). C866-74.
[36] S.V. Raju, V.Y. Lin, L. Liu, C.M. McNicholas, S. Karki, P.A. Sloane, L. Tang, P. L. Jackson, W. Wang, L. Wilson, K.J. Macon, M. Mazur, J.C. Kappes, L.J. DeLucas, S. Barnes, K. Kirk, G.J. Tearney, S.M. Rowe, The cystic fibrosis transmembrane conductance regulator potentiator ivacaftor augments mucociliary clearance abrogating cystic fibrosis transmembrane conductance regulator inhibition by cigarette smoke, Am. J. Respir. Cell Mol. Biol. 56 (1) (2017) 99–108.
[37] S. Mukhopadhyay, J.R. Hoidal, T.K. Mukherjee, Role of TNFα in pulmonary pathophysiology, Respir. Res. 7 (1) (2006) 125.
[38] T.L. Bonfield, J.R. Panuska, M.W. Konstan, K.A. Hilliard, J.B. Hilliard, H. Ghnaim, M. Berger, Inflammatory cytokines in cystic fibrosis lungs, Am. J. Respir. Crit. Care Med 152 (6 Pt 1) (1995), 2111-8.
[39] S.M. Rowe, S.L. Heltshe, T. Gonska, S.H. Donaldson, D. Borowitz, D. Gelfond, S. D. Sagel, U. Khan, N. Mayer-Hamblett, J.M. Van Dalfsen, E. Joseloff, B.W. Ramsey, Clinical mechanism of the cystic fibrosis transmembrane conductance regulator potentiator ivacaftor in G551D-mediated cystic fibrosis, Am. J. Respir. Crit. Care Med 190 (2) (2014), 175-84.
[40] K.B. Hisert, T.P. Birkland, K.Q. Schoenfelt, M.E. Long, B. Grogan, S. Carter, W. C. Liles, E.F. McKone, L. Becker, A.M. Manicone, Ivacaftor decreases monocyte sensitivity to interferon-γ in people with cystic fibrosis, ERJ Open Res 6 (2) (2020).
[41] D.o.H. Australian Government, Australian Public Assessment Report for Lumacaftor/Ivacaftor, (2016).
[42] J. Guan, H. Yuan, S. Yu, S. Mao, Q. Tony Zhou, Spray dried inhalable ivacaftor co-amorphous microparticle formulations with leucine achieved enhanced in vitro dissolution and superior aerosol performance, Int. J. Pharm. 622 (2022), 121859.
[43] S. Zhang, C.L. Shrestha, B.T. Kopp, Cystic fibrosis transmembrane conductance regulator (CFTR) modulators have differential effects on cystic fibrosis macrophage function, Sci. Rep. 8 (1) (2018) 17066.
[44] E.M. Bruscia, P.X. Zhang, E. Ferreira, C. Caputo, J.W. Emerson, D. Tuck, D. S. Krause, M.E. Egan, Macrophages directly contribute to the exaggerated inflammatory response in cystic fibrosis transmembrane conductance regulator-/- mice, Am. J. Respir. Cell Mol. Biol. 40 (3) (2009) 295–304.
[45] K.H. Harwood, R.M. McQuade, A. Jarnicki, E.K. Schneider-Futschik, Ivacaftor alters macrophage and lymphocyte infiltration in the lungs following lipopolysaccharide exposure, ACS Pharmacol. Transl. Sci. 5 (6) (2022) 419–428.
[46] J.E. Hoppe, B.D. Wagner, J. Kirk Harris, S.M. Rowe, S.L. Heltshe, E.M. DeBoer, S. D. Sagel, Effects of ivacaftor on systemic inflammation and the plasma proteome in people with CF and G551D, J. Cyst. Fibros. 21 (6) (2022) 950–958.
[47] Y. Fujita, T. Yamashita, The roles of RGMa-neogenin signaling in inflammation and angiogenesis, Inflamm. Regen. 37 (1) (2017) 6.
[48] F. Kronenberg, B. Kollerits, S. Kiechl, C. Lamina, L. Kedenko, C. Meisinger, J. Willeit, C. Huth, G. Wietzorrek, M.E. Altmann, B. Thorand, A. Melmer, D. Dähnhardt, P. Santer, W. Rathmann, B. Paulweber, W. Koenig, A. Peters, I. M. Adham, H. Dieplinger, Plasma concentrations of afamin are associated with the prevalence and development of metabolic syndrome, Circ. Cardiovasc. Genet. 7 (6) (2014) 822–829.
[49] M. Delgado, D. Ganea, Vasoactive intestinal peptide and pituitary adenylate cyclase-activating polypeptide inhibit antigen-induced apoptosis of mature T lymphocytes by inhibiting fas ligand expression1, J. Immunol. 164 (3) (2000) 1200–1210.
[50] M. DELGADO, C. ABAD, C. MARTINEZ, M.G. JUARRANZ, J. LECETA, D. GANEA, R.P. GOMARIZ, PACAP in Immunity and Inflammation, Ann. N. Y. Acad. Sci. 992 (1) (2003) 141–157.
[51] Z. Gao, X. Su, CFTR regulates acute inflammatory responses in macrophages, QJM Int. J. Med. 108 (12) (2015) 951–958.
[52] T.L. Bonfield, C.A. Hodges, C.U. Cotton, M.L. Drumm, Absence of the cystic fibrosis transmembrane regulator (Cftr) from myeloid-derived cells slows resolution of inflammation and infection, J. Leukoc. Biol. 92 (5) (2012), 1111-22.
[53] A. Di, M.E. Brown, L.V. Deriy, C. Li, F.L. Szeto, Y. Chen, P. Huang, J. Tong, A. P. Naren, V. Bindokas, H.C. Palfrey, D.J. Nelson, CFTR regulates phagosome acidification in macrophages and alters bactericidal activity, Nat. Cell Biol. 8 (9) (2006) 933–944.
[54] J.C. Phipps, D.M. Aronoff, J.L. Curtis, D. Goel, E. O'Brien, P. Mancuso, Cigarette smoke exposure impairs pulmonary bacterial clearance and alveolar macrophage complement-mediated phagocytosis of Streptococcus pneumoniae, Infect. Immun. 78 (3) (2010), 1214-20.
[55] I. Ni, C. Ji, N. Vij, Second-hand cigarette smoke impairs bacterial phagocytosis in macrophages by modulating CFTR dependent lipid-rafts, PLoS One 10 (3) (2015), e0121200.
[56] M.P. Boyle, S.C. Bell, M.W. Konstan, S.A. McColley, S.M. Rowe, E. Rietschel, X. Huang, D. Waltz, N.R. Patel, D. Rodman, A CFTR corrector (lumacaftor) and a CFTR potentiator (ivacaftor) for treatment of patients with cystic fibrosis who have a phe508del CFTR mutation: a phase 2 randomised controlled trial, Lancet Respir. Med 2 (7) (2014), 527-38.
[57] C.E. Wainwright, J.S. Elborn, B.W. Ramsey, G. Marigowda, X. Huang, M. Cipolli, C. Colombo, J.C. Davies, K. De Boeck, P.A. Flume, M.W. Konstan, S.A. McColley, K. McCoy, E.F. McKone, A. Munck, F. Ratjen, S.M. Rowe, D. Waltz, M.P. Boyle, Lumacaftor-Ivacaftor in Patients with Cystic Fibrosis Homozygous for Phe508del CFTR, N. Engl. J. Med 373 (3) (2015), 220-31.
[58] R. Barnaby, K. Koeppen, A. Nymon, T.H. Hampton, B. Berwin, A. Ashare, B. A. Stanton, Lumacaftor (VX-809) restores the ability of CF macrophages to phagocytose and kill Pseudomonas aeruginosa, Am. J. Physiol. Lung Cell Mol. Physiol. 314 (3) (2018) L432–l438.
[59] K.H. Harwood, R.M. McQuade, A. Jarnicki, E.K. Schneider-Futschik, Anti-inflammatory influences of cystic fibrosis transmembrane conductance regulator drugs on lung inflammation in cystic fibrosis, Int J. Mol. Sci. 22 (14) (2021).